Ferroelectric phase transitions and off-centre displacements in systems with strong electron-phonon interaction

1999 J. Phys.: Condens. Matter 11 9807

(http://iopscience.iop.org/0953-8984/11/48/337)

J. Phys.: Condens. Matter **11** (1999) 9807–9822. Printed in the UK PII: S0953-8984(99)05806-3

Ferroelectric phase transitions and off-centre displacements in systems with strong electron–phonon interaction

Yakov Girshberg and Yizhak Yacoby
Racah Institute of Physics, Hebrew University, Jerusalem 91904, Israel

Received 8 July 1999, in final form 16 September 1999

Abstract. We present a microscopic theory of ferroelectric phase transitions and off-centre displacements in perovskites. We show that the inclusion of strong intraband electron–phonon interaction (i.e. the existence of small polarons) into the framework of the interband theory of displacive-like ferroelectrics leads to local spin-like structural distortions in the paraelectric phase. Their interaction with the soft mode induces spin–spin coupling through the soft phonon leading to a spin-ordering phase transition. The resulting theory is shown to quantitatively explain both displacive-like and order–disorder-like features of two representative perovskites: $KNbO_3$ and $PbTiO_3$.

1. Introduction

For a long time, in fact since the discovery of ferroelectricity in perovskites, perovskite ferroelectrics ($BaTiO_3$, $PbTiO_3$, $KNbO_3$) have been considered as exemplary displacive ferroelectrics [1,2]. However, various experimental results were found to be not quite consistent with pure displacive-type models. The existence of strong diffuse x-ray scattering [3–5] in the cubic, tetragonal and orthorhombic phases suggested that the metal atoms are displaced along [111]-type directions in all of these phases. Raman and differential Raman [6–8] experiments on pure and mixed crystals showed that the Raman selection rules are violated in the cubic phase, suggesting the existence of disordered local distortions in the paraelectric phase. IR [9], Raman [10] and neutron scattering [11] measurements showed that the soft-mode frequency does not vanish as T approaches T_C, but saturates at a finite value. Finally, the existence and temperature dependence of the central peak in *pure* oxygen perovskite crystals [12, 13] is easily understood in order–disorder-type transitions, but is not expected in pure displacive-like transitions.

The temperature dependence of the local distortions in the cubic phase has been directly measured by x-ray absorption fine-structure (XAFS) experiments on various pure and mixed perovskites [14–18]. The experiments showed that in $KNbO_3$ the Nb ions are indeed displaced in [111]-type directions, whereas in $PbTiO_3$ the Ti and Pb are displaced in [100]-type directions even at temperatures which are hundreds of degrees above T_C. The local distortions are large—more than 40% of the displacements at $T = 0$ K. Furthermore, XAFS studies provided the position pair distribution function between the probe and its nearest neighbours. In all cases the function was found to be double peaked even far above T_C, with a minimum at a distance that corresponds to the ideal cubic structure. It is important to note that XAFS showed that, in contrast to these materials, Ta and Ti in the incipient ferroelectrics $KTaO_3$ [17] and $SrTiO_3$ [19] are not displaced.

0953-8984/99/489807+16$30.00

On the other hand, a number of the fundamental characteristics of the ferroelectric perovskites may be understood only in the framework of pure displacive-like phase transitions. For all perovskites the static permittivity $\varepsilon(T)$ satisfies a Curie–Weiss law with a Curie–Weiss constant $C = (1\text{–}3) \times 10^5$ K, which is typical of displacive-type transitions only. In order–disorder-type transitions this constant is always more than two orders of magnitude smaller. For all oxygen perovskites one observes the existence of a soft mode above T_C. In contrast, in an order–disorder transition there is no soft mode in the paraelectric phase if tunnelling is neglected. In all high-temperature ferroelectric perovskites the transition from the paraelectric to the ferroelectric phase is always first order with $T_P - T_C$ and of the order of 10–60 K, typical for displacive-type transitions. In order–disorder-type transitions the difference is usually under 1 K.

In conclusion, the experimental results show that perovskite ferroelectrics display both displacive and order–disorder-like properties. The existence of local distortions seems to be a very general property. Large local distortions in the cubic phase were observed not only in perovskites undergoing ferroelectric transitions but also in perovskites undergoing antiferroelectric [20] and antiferrodistortive [21] transitions.

Most of the theoretical work on ferroelectric phase transitions in perovskites assumes that the transition is purely displacive. The models are either 'pure' phonon ones [2, 22–24], or models based on the interband electron–phonon interaction [25–28]. These models treat the origin and temperature dependence of the critical vibration both below and above T_C, but ignore the existence of the local lattice distortions in the high-symmetry phase and their effect on the phase transition. Consequently, they do not account for many of the experimental results mentioned above. The possibility of local distortions in the cubic phase has been discussed only in a number of papers based on molecular orbital calculations for an MO_6 octahedron (where M is a metal ion) [29] and in computer simulations of one- or two-dimensional non-linear models [30, 31]. However, these works do not discuss any causal relationship between the local distortions, the soft mode and the phase transition.

During the last ten years various properties associated with the structural phase transition of perovskite crystals were calculated using first-principles calculation methods [32–36]. However, by their very nature, these methods do not provide analytical relations among the various parameters and phenomena involved in these structural phase transitions. Such relations are important if one is to gain a physical insight into the problem.

In a recent paper [37] we discussed a phenomenological model of phase transitions in perovskites which is based on the following assumptions:

(a) The metal ions undergo spontaneous off-centre displacements (the pseudospin subsystem).
(b) The system has a soft mode, which could lead to a purely displacive phase transition.
(c) The off-centre displacements and the soft mode interact with each other.

Within the framework of this model, a non-trivial phase transition of the order–disorder type takes place in the system: the spin–spin interaction is mediated by the soft mode, leading to spin ordering and phase transition.

We have shown that this model accounts quantitatively for the large Curie–Weiss constant, the temperature dependence of the soft mode, the difference between the transition temperature and the temperature at which the square of the soft mode extrapolates to zero, the temperature dependence of the height and width of the central peak and the temperature and frequency dependence of the imaginary part of the dielectric constant. The comparison was made for two materials with quite different properties, $KNbO_3$ and $PbTiO_3$.

In this work, we propose a micro-theory of ferroelectric phase transitions which explains the origin of the off-centre displacements, the soft mode and their coupling in terms of two

types of strong electron–phonon interaction.

We extend the interband theory of ferroelectricity [25–28] by including, in addition to the conventional strong interband electron–transverse optical phonon interaction that leads to the existence of a soft mode, a strong intraband electron–longitudinal optical phonon interaction. We know that this interaction is strong because ferroelectric perovskites have polaronic mobilities [38–41]. We show that this additional interaction leads to the existence of spontaneous local structural distortions in the paraelectric phase and allows us to calculate in a fully coherent way the temperature dependence of the soft mode, the size of the local distortions and the coupling between them. We show that the calculated values are in good agreement with the parameters found in our previous work and therefore quantitatively explain both the displacive-like and order–disorder-like properties observed experimentally in these systems. Furthermore, this theory explains why crystals that have polaronic mobility ($BaTiO_3$ [38, 39], $PbTiO_3$ [40], $KNbO_3$ [40, 41]) have off-centre displacements, whereas the incipient ferroelectrics ($SrTiO_3$ and $KTaO_3$) that have ordinary band mobility [42, 43] have no off-centre displacements.

2. The system Hamiltonian, instability and soft mode in a strong-coupling system

We consider a system with a Hamiltonian H, which includes a two-band electron Hamiltonian H_e, a free-phonon-field Hamiltonian H_{ph} and an electron–phonon interaction Hamiltonian H_{e-ph}:

$$H = H_e + H_{ph} + H_{e-ph}. \tag{1}$$

In the presence of strong intraband electron–phonon coupling and narrow electronic bands, the polarization of the lattice by the electrons (polaron effect) becomes important and the single-electron band states (electronic momentum or $\boldsymbol{p}$-representation) do not constitute a good initial system of functions [44]. Therefore we represent the electronic part of the Hamiltonian in a more convenient site representation:

$$H_e = \sum_{\boldsymbol{m},\alpha} \varepsilon_{\alpha\boldsymbol{m}} a^+_{\alpha\boldsymbol{m}} a_{\alpha\boldsymbol{m}} + \sum_{\boldsymbol{m},\boldsymbol{m}',\alpha} J_{\alpha\alpha}(\boldsymbol{m}-\boldsymbol{m}') a^+_{\alpha\boldsymbol{m}} a_{\alpha\boldsymbol{m}'} \tag{2}$$

where α takes the values 1 and 2 for the conduction band and valence band respectively, $\boldsymbol{m}$ labels the site (the corresponding lattice vector), the summation over $\boldsymbol{m}$ is the summation over all unit cells, $J_{\alpha\alpha}(\boldsymbol{m}-\boldsymbol{m}')$ denotes the bare overlap integral and $a^+_{\alpha\boldsymbol{m}}$ ($a_{\alpha\boldsymbol{m}}$) is the $(\boldsymbol{m},\alpha)$-site creation (annihilation) electron operator.

The initial overlap integral between the nearest neighbours $J_{\alpha\alpha}$ is assumed to be small, i.e. $J_{\alpha\alpha}/E_{p\alpha} < 1$, where $E_{p\alpha}$ is the polaron level shift (see below). In addition, we assume that $E_{p\alpha}/E_g < 1$, where the band gap $E_g = \varepsilon_1 - \varepsilon_2$. In this case [44] the polaron effect does not lead to an entanglement of the initial single-electron states.

As a rule, the strongest intraband electron–phonon interaction in ionic crystals is the interaction with longitudinal polar vibrations, whereas the soft mode is due to interband interaction with the transverse polar optical vibration. We therefore include in the free-phonon Hamiltonian two terms:

$$H_{ph} = \sum_{\boldsymbol{q}} \omega_{\boldsymbol{q}l} b^+_{\boldsymbol{q}l} b_{\boldsymbol{q}l} + \sum_{\boldsymbol{q}} \omega_{\boldsymbol{q}t} b^+_{\boldsymbol{q}t} b_{\boldsymbol{q}t} \tag{3}$$

where subscripts l and t label the longitudinal and transverse branch respectively, $\omega_{\boldsymbol{q}}$ represents the phonon frequency and $b^+_{\boldsymbol{q}}$ ($b_{\boldsymbol{q}}$) are the phonon creation (annihilation) operators with wave vector $\boldsymbol{q}$.

Finally, the electron–phonon interaction Hamiltonian consists of strong intraband and interband Fröhlich (linear in the displacements) terms:

$$H_{e-ph} = H^{l}_{e-ph} + H^{t}_{e-ph} \tag{4}$$

$$H^{l}_{e-ph} = \frac{1}{\sqrt{2N}} \sum_{q,m,\alpha} \omega_{ql}[\gamma^{*}_{q\alpha} \exp(-\mathrm{i}\boldsymbol{q}\cdot\boldsymbol{m}) b^{+}_{ql} + \gamma_{q\alpha} \exp(\mathrm{i}\boldsymbol{q}\cdot\boldsymbol{m}) b_{ql}] a^{+}_{\alpha m} a_{\alpha m} \tag{5}$$

$$H^{t}_{e-ph} = \frac{1}{\sqrt{N}} \sum_{q,m,\alpha,\beta,\alpha\neq\beta} \Gamma_{\alpha\beta}(\boldsymbol{q}) \sqrt{\frac{\omega_{qt}}{2}} \exp(\mathrm{i}\boldsymbol{q}\cdot\boldsymbol{m})[b_{qt} + b^{+}_{-qt}] a^{+}_{\alpha m} a_{\beta m} \tag{6}$$

where $\gamma_{q\alpha}$ and $\Gamma_{\alpha\beta}(\boldsymbol{q})$ are the corresponding electron–phonon coupling constants and N is the number of states in the band. This Hamiltonian differs from the usual interband ferroelectricity Hamiltonian [27] in that it contains, in addition, the intraband electron–phonon interaction. We assume that this interaction is strong, which is mathematically equivalent to the inequality [45]

$$\overline{\gamma}_{\alpha} \equiv \frac{1}{2N} \sum_{q} |\gamma_{q\alpha}|^{2} \gg 1. \tag{7}$$

The coupling constant $\Gamma_{\alpha\beta} \sim d_{\alpha\beta}$, where $d_{\alpha\beta}$ is the direct allowed interband dipole matrix element. It depends, only weakly, on the wave vectors [27] and is assumed to be a constant: $\Gamma_{\alpha\beta}(\boldsymbol{q}) = \Gamma_{\alpha\beta} = \Gamma_{\beta\alpha} \equiv \Gamma = \text{constant}$.

The strong intraband electron–phonon coupling cannot be treated by perturbation. We therefore use the following Lang–Firsov canonical transformation [44, 45]:

$$\widetilde{H} = \exp(-S) H \exp(S) \equiv \widetilde{H}_{e} + \widetilde{H}_{ph} + \widetilde{H}^{l}_{e-ph} + \widetilde{H}^{t}_{e-ph} \tag{8}$$

$$S = \sum_{m,\alpha} S_{\alpha m} a^{+}_{\alpha m} a_{\alpha m} \tag{9}$$

$$S_{\alpha m} = \frac{1}{\sqrt{2N}} \sum_{q} [b^{+}_{ql}\gamma^{*}_{q\alpha} \exp(-\mathrm{i}\boldsymbol{q}\cdot\boldsymbol{m}) - b_{ql}\gamma_{q\alpha} \exp(\mathrm{i}\boldsymbol{q}\cdot\boldsymbol{m})] \tag{10}$$

which allows us to include the principal part of the intraband interaction equation (5) in the zeroth-order Hamiltonian and to diagonalize it exactly. We define a set of new electron and phonon operators as follows:

$$a^{+}_{\alpha m} = \widetilde{a}^{+}_{\alpha m} \exp\left[-\frac{1}{\sqrt{2N}} \sum_{q} (b^{+}_{-ql}\gamma^{*}_{-q\alpha} - b_{ql}\gamma_{q\alpha}) \mathrm{e}^{\mathrm{i}q\cdot m} \right] \tag{11}$$

$$b^{+}_{ql} = \widetilde{b}^{+}_{ql} - \frac{1}{\sqrt{2N}} \sum_{m,\alpha} a^{+}_{\alpha m} a_{\alpha m} \gamma_{q\alpha} \exp(\mathrm{i}\boldsymbol{q}\cdot\boldsymbol{m}). \tag{12}$$

In terms of these operators, after some transformations we have

$$\widetilde{H}_{e} = \sum_{\alpha,m} (\varepsilon_{\alpha} - E_{p\alpha}) \widetilde{a}^{+}_{\alpha m} \widetilde{a}_{\alpha m} + \sum_{\alpha,m,m'} J_{\alpha\alpha}(\boldsymbol{m}-\boldsymbol{m}') \langle F_{\alpha\alpha}(\boldsymbol{m}-\boldsymbol{m}') \widetilde{a}^{+}_{\alpha m} \widetilde{a}_{\alpha m'}$$
$$- \frac{1}{2N} \sum_{m\neq m',\alpha,\alpha'} (\gamma^{*}_{q\alpha}\gamma_{q\alpha'}) \mathrm{e}^{\mathrm{i}q\cdot(m-m')} \widetilde{a}^{+}_{\alpha m} \widetilde{a}_{\alpha m} \widetilde{a}^{+}_{\alpha' m'} \widetilde{a}_{\alpha' m'} \tag{13}$$

$$\widetilde{H}_{ph} = \sum_{q} \omega_{ql} \widetilde{b}^{+}_{ql} \widetilde{b}_{ql} + \sum_{q} \omega_{qt} b^{+}_{qt} b_{qt} \tag{14}$$

$$\widetilde{H}^{t}_{e-ph} = \sum_{m,q,\alpha\neq\beta} \Gamma_{\alpha\beta}(\boldsymbol{q}) \sqrt{\frac{\omega_{qt}}{2N}} F_{\alpha\beta}(\boldsymbol{m}) \mathrm{e}^{\mathrm{i}q\cdot m} (b_{qt} + b_{-qt}) \widetilde{a}^{+}_{\alpha m} \widetilde{a}_{\beta m} \tag{15}$$

where

$$E_{p\alpha} = \frac{1}{2N} \sum_{q} \omega_{ql} |\gamma_{q\alpha}|^{2} \tag{16}$$

is the polaron level shift and $F_{\alpha\alpha}(\boldsymbol{m},\boldsymbol{m}')$ and $F_{\alpha\beta}(\boldsymbol{m})$ are the multiphonon operators:

$$F_{\alpha\alpha}(\boldsymbol{m},\boldsymbol{m}')=\exp\left\{\frac{1}{\sqrt{2N}}\sum_{\boldsymbol{q}}[b^{+}_{\boldsymbol{q}l}\gamma^{*}_{\boldsymbol{q}\alpha}(\mathrm{e}^{-\mathrm{i}\boldsymbol{q}\cdot\boldsymbol{m}}-\mathrm{e}^{-\mathrm{i}\boldsymbol{q}\cdot\boldsymbol{m}'})-b_{\boldsymbol{q}l}\gamma_{\boldsymbol{q}\alpha}(\mathrm{e}^{\mathrm{i}\boldsymbol{q}\cdot\boldsymbol{m}}-\mathrm{e}^{\mathrm{i}\boldsymbol{q}\cdot\boldsymbol{m}'})]\right\} \tag{17}$$

$$F_{\alpha\beta}(\boldsymbol{m})\Big|_{(\alpha\neq\beta)}=\exp\left\{\frac{1}{\sqrt{2N}}\sum_{\boldsymbol{q}}[b^{+}_{\boldsymbol{q}l}(\gamma^{*}_{\boldsymbol{q}\alpha}-\gamma^{*}_{\boldsymbol{q}\beta})\mathrm{e}^{-\mathrm{i}\boldsymbol{q}\cdot\boldsymbol{m}}-b_{\boldsymbol{q}l}(\gamma_{\boldsymbol{q}\alpha}-\gamma_{\boldsymbol{q}\beta})\mathrm{e}^{\mathrm{i}\boldsymbol{q}\cdot\boldsymbol{m}}]\right\}. \tag{18}$$

In the usual treatment of small polarons [45], the operator $F_{\alpha\alpha}(\boldsymbol{m},\boldsymbol{m}')$ describes processes of multiphonon absorption and emission. These processes are related to the local dynamical deformation of the lattice, as the electron moves (jumps) from site to site. Here the electronic transitions are between identical states (α) at different sites ($\boldsymbol{m}\neq\boldsymbol{m}'$). The operator $F_{\alpha\beta}(\boldsymbol{m})$ is absent in the ordinary small-polaron theory and appears only if the interband interaction is taken into account. Like $F_{\alpha\alpha}(\boldsymbol{m},\boldsymbol{m}')$, the operator $F_{\alpha\beta}(\boldsymbol{m})$ describes multiphonon processes associated with the local deformation of the lattice due to a jump of the electron from state to state ($\alpha\neq\beta$) on the same site.

In the $\boldsymbol{p}$-representation the first two terms of $\widetilde{H}_e$ may be written in the form

$$\widetilde{H}_0=\sum_{\alpha,\boldsymbol{p}}\widetilde{\varepsilon}_{\alpha}(\boldsymbol{p})\widetilde{a}^{+}_{\alpha\boldsymbol{p}}\widetilde{a}_{\alpha\boldsymbol{p}} \tag{19}$$

where

$$\widetilde{\varepsilon}_{\alpha}(\boldsymbol{p})=\varepsilon_{\alpha}-E_{p\alpha}+\sum_{\boldsymbol{m},\boldsymbol{m}'}J_{\alpha\alpha}(\boldsymbol{m}-\boldsymbol{m}')\langle F_{\alpha\alpha}\rangle\mathrm{e}^{\mathrm{i}\boldsymbol{p}\cdot(\boldsymbol{m}-\boldsymbol{m}')} \tag{20}$$

is the narrow polaron band and the average of $F_{\alpha\alpha}(\boldsymbol{m},\boldsymbol{m}')$ is given by [45]

$$\langle F_{\alpha\alpha}(\boldsymbol{m}-\boldsymbol{m}')\rangle=\exp\left\{-\frac{1}{2N}\sum_{\boldsymbol{q}}|\gamma_{\boldsymbol{q}\alpha}|^{2}[1-\cos\boldsymbol{q}\cdot(\boldsymbol{m}-\boldsymbol{m}')]\coth\frac{\omega_{\boldsymbol{q}l}}{2T}\right\}\ll 1. \tag{21}$$

The last term in equation (13) describes the direct residual interaction between two electrons at different sites ($\boldsymbol{m}\neq\boldsymbol{m}'$). In the cases of polaronic superconductors [46] and in the polaronic theory of metal–insulator transition [47] this interaction is crucial. However, in our problem, it is inessential and may be left out. The residual intraband polaron–phonon interaction $\widetilde{H}^{l}_{e-ph}$ becomes proportional to the small overlap integral $J_{\alpha\alpha}(\boldsymbol{m}-\boldsymbol{m}')$ and may be taken into account by perturbation theory. This interaction plays the principal role in the theory of kinetic effects in polaron semiconductors and in the theory of polaron superconductivity (side by side with the direct polaron–polaron interaction). In our case the corrections associated with it are smaller by a factor of $(J_{\alpha\alpha}/E_g)^2\ll 1$ relative to the background of interband interaction $\widetilde{H}^{t}_{e-ph}$ and may therefore be left out too.

Thus, taking into account the strong intraband electron–phonon interaction leads, in our problem, to changes in the atomic equilibrium positions (see equation (12)), to the strong narrowing of the electron (polaron) bands (see equation (20)) and to the renormalization of the interband interaction—that is, to the appearance of the operator $F_{\alpha\beta}(\boldsymbol{m})$ in $\widetilde{H}^{t}_{e-ph}$ (equation (15)). Finally, the transformed Hamiltonian may be written in the following form:

$$\widetilde{H}=\widetilde{H}_0+\widetilde{H}_{ph}+\widetilde{H}^{t}_{e-ph}. \tag{22}$$

We now consider the origin of the dynamical lattice instability associated with sufficiently strong interband interaction $\widetilde{H}^{t}_{e-ph}$. In the following we use the temperature diagram technique [48] and express the operators in the Matsubara representation.

The renormalized phonon spectrum defined by the Hamiltonian, equation (22), is given by the poles of the full phonon Green's function $D(\boldsymbol{q},\omega_n)$. In general it satisfies Dyson's equation

$$D(\boldsymbol{q},\omega_n)=D_0(\boldsymbol{q},\omega_n)+D_0\Pi D. \tag{23}$$

If all perturbing operators satisfy Wick's theorem and to all orders of perturbation there are both irreducible and reducible diagrams, the equation is soluble. Here $D_0(\boldsymbol{q}, \omega_n)$ is the zeroth (free) Green's function which corresponds to the free-phonon Hamiltonian $\widetilde{H}_{ph}$ and Π is the total polarization operator of the system.

If $\gamma_{q\alpha}$ is small or zero ($\overline{\gamma}_\alpha \ll 1$, $F_{\alpha\beta}(\boldsymbol{m}, \tau) = 1$), Π can be evaluated as in the usual interband theory of ferroelectricity [27, 28], leading to the existence of the soft mode.

In the present case ($\overline{\gamma}_\alpha \gg 1$) the situation is quite different. To all orders of perturbation the diagrams contain averages of electronic, phononic and $F_{\alpha\beta}(\boldsymbol{m}, \tau)$ operators. Since the different types of operator commute with each other, the averages can be calculated separately for operators of different types. Due to Wick's theorem, the averages of the electron and phonon operators can be related to the electronic and phononic Green's functions respectively. However, for $F_{\alpha\beta}(\boldsymbol{m}, \tau)$ operators Wick's theorem does not hold, leading to the irreducibility of all diagrams to all orders of perturbation for the phonon and electron Green's functions. Therefore Dyson's equation is not soluble directly. However, using the considerable difference between the actual values of the internal electronic, phononic and multiphonon correlator frequencies (for more details see the appendix), the polarization operator Π can be calculated and, from it, the soft-mode frequency:

$$\Omega^2_{q\to 0,t} = \omega^2_{q\to 0,t}\left[\widetilde{\Delta}_0 + \frac{3}{2}\frac{\overline{\omega}}{2\overline{E}}\coth\left(\frac{\overline{\omega}}{2T}\right)\right] \tag{24}$$

where $\overline{\omega}$ is the average of the soft-mode phonon branch energy,

$$\frac{1}{\overline{E}} \equiv \frac{1}{N}\sum_{\boldsymbol{p}}\frac{1}{\widetilde{\varepsilon}_1(\boldsymbol{p}) - \widetilde{\varepsilon}_2(\boldsymbol{p})} \tag{25}$$

and

$$\widetilde{\Delta}_0 \equiv \left[1 - \frac{4\Gamma^2}{\overline{E}} - \left(\frac{E_p}{\overline{E}}\right)^2\right]. \tag{26}$$

In deriving equation (24) we have assumed, as usual [25–27], that $|\widetilde{\Delta}_0| \ll 1$. This is the threshold inequality that binds the coupling constant $\Gamma_{\alpha\beta}$ from below. If $\widetilde{\Delta}_0 \leq 0$, the system may undergo a displacive-like phase transition at $T = \widetilde{T}_0$, such that $\Omega_{\boldsymbol{q}=0t}(\widetilde{T}_0) = 0$. Close to $\widetilde{T}_0$ (for $\widetilde{T}_0 > \overline{\omega}$),

$$\Omega^2_{0t} = \omega^2_{0t}|\widetilde{\Delta}_0|[(T - \widetilde{T}_0)/\widetilde{T}_0] = A(T - \widetilde{T}_0) \tag{27}$$

$$A = \frac{3}{2}\left(\frac{\omega^2_{0t}}{2\overline{E}}\right)\left(\frac{\omega^2_{0t}}{\overline{\omega}^2}\right) \qquad \widetilde{T}_0 = \frac{2}{3}\left(\frac{\overline{\omega}}{\omega_{0t}}\right)^2|\widetilde{\Delta}_0|\overline{E}. \tag{28}$$

So, at first sight, the presence of the strong intraband interaction does not change qualitatively the dynamics of the phase transition: we have, as usual, a soft mode, equation (27), that leads to a displacive-like phase transition at $T = \widetilde{T}_0$.

However, so far we have investigated only the effect of the strong intraband electron–phonon coupling on the electron subsystem: that is, we replaced the electrons by polarons, the interband electron–transverse phonon interaction by a polaron–transverse phonon interaction and introduced $F_{\alpha\beta}(\boldsymbol{m})$ in the expression for $\widetilde{H}^t_{e-ph}$ (equation (15)). We shall now investigate the change in the phonon subsystem, which also results from this interaction. As shown below, the phonon reconstruction, in the presence of interband interactions, leads to off-centre displacements of the active ions, which qualitatively change the phase transition picture.

3. Off-centre displacements and the ferroelectric phase transition

In general the displacement operator of the jth ion in the $\boldsymbol{m}$th unit cell is given by

$$\boldsymbol{r}_{jm} = \frac{1}{\sqrt{N}} \sum_{\boldsymbol{q},s} \sqrt{\frac{1}{2M^*\omega_{\boldsymbol{q}s}}} [\boldsymbol{e}^j_{\boldsymbol{q}s} \exp(\mathrm{i}\boldsymbol{q}\cdot\boldsymbol{m}) b_{\boldsymbol{q}s} + \boldsymbol{e}^{j*}_{\boldsymbol{q}s} \exp(-\mathrm{i}\boldsymbol{q}\cdot\boldsymbol{m}) b^+_{\boldsymbol{q}s}] \quad (29)$$

where s is the branch number, M^* is the reduced unit-cell mass and $\boldsymbol{e}^j_{\boldsymbol{q}s}$ is the polarization unit vector of the corresponding mode. The $s = l$ phonon branch has changed due to the strong intraband electron–phonon interaction and is given by equation (12). Substituting it in equation (29) we obtain in the homopolar approximation a new displacement operator

$$\boldsymbol{R}_{jm} = \sum_{\boldsymbol{q},s} \sqrt{\frac{1}{2M^*\omega_{\boldsymbol{q}s}N}} \boldsymbol{e}^j_{\boldsymbol{q}s} \exp(\mathrm{i}\boldsymbol{q}\cdot\boldsymbol{m})[b_{\boldsymbol{q}s} + b^+_{-\boldsymbol{q}s}] + \boldsymbol{b}_{jm} \quad (30)$$

$$\boldsymbol{b}_{jm} = \frac{1}{N} \sum_{\boldsymbol{q}} \sqrt{\frac{2}{M^*\omega_{\boldsymbol{q}l}}} \boldsymbol{e}^j_{\boldsymbol{q}l} \exp(\mathrm{i}\boldsymbol{q}\cdot\boldsymbol{m})\gamma^*_{\boldsymbol{q}12} \times \sum_{\boldsymbol{m}'} \exp(-\mathrm{i}\boldsymbol{q}\cdot\boldsymbol{m}')\widetilde{a}^+_{1\boldsymbol{m}'}\widetilde{a}_{1\boldsymbol{m}'} \qquad \gamma_{\boldsymbol{q}\alpha\beta} \equiv (\gamma_{\boldsymbol{q}\alpha} - \gamma_{\boldsymbol{q}\beta}). \quad (31)$$

The first term in equation (30) contains only phonon operators, representing the usual vibrations about a new position. The second term $\boldsymbol{b}_{jm}$ contains only electronic operators and represents a spontaneous local off-centre displacement, which is proportional to the intraband electron–phonon interaction constant.

Due to symmetry, the average of the vector $\boldsymbol{b}_{jm}$ is zero in the cubic phase. However, the average of $|\boldsymbol{b}_{jm}|^2$ is not zero and is given by

$$|\boldsymbol{b}_{jm}|^2 = \frac{1}{N} \sum_{\boldsymbol{q}} \frac{2\omega_{\boldsymbol{q}l}}{M^*\omega^2_{\boldsymbol{q}l}} |e^j_{\boldsymbol{q}s}|^2 |\gamma_{\boldsymbol{q}12}|^2 \left(\frac{N_e}{N}\right) \quad (32)$$

where N_e/N is the electron density. Notice that $|\boldsymbol{b}_{jm}|^2$ is independent of $\boldsymbol{m}$ and is set to $|\boldsymbol{b}_{jm}|^2 \equiv |\boldsymbol{b}_j|^2$.

The electron density can be expressed [48] in terms of the electron Green's function $G_{\alpha\alpha}(\boldsymbol{p}, \varepsilon_n)$:

$$N_e/N = (T/N) \sum_{\boldsymbol{p},\varepsilon_n}, G_{11}(\boldsymbol{p}, \varepsilon_n) \quad (33)$$

which, in view of the interband electron–phonon Hamiltonian, equation (15), may be written in the form

$$G_{\alpha\alpha}(\boldsymbol{p}, \varepsilon_n) = G^{(0)}_{\alpha\alpha}(\boldsymbol{p}, \varepsilon_n) + \frac{T^2}{N} \sum_{\boldsymbol{q},\omega_n,\nu_n} G^{(0)}_{\alpha\alpha}(\boldsymbol{p}, \varepsilon_n)\Gamma_{\alpha\beta}\Phi_{\alpha\beta}(\nu_n)D(\boldsymbol{q}, \omega_n) \times G_{\beta\beta}(\boldsymbol{p}-\boldsymbol{q}, \varepsilon_n - \omega_n - \nu_n)\Gamma_{\beta\alpha}G_{\alpha\alpha}(\boldsymbol{p}, \varepsilon_n) \quad (34)$$

where

$$G^{(0)}_{\alpha\alpha}(\boldsymbol{p}, \varepsilon_n) = [\mathrm{i}\varepsilon_n - \widetilde{\varepsilon}_\alpha(\boldsymbol{p})]^{-1} \quad (35)$$

is the free-electron Green's function.

After some transformations we get

$$N_e/N = 2\sum_{\boldsymbol{p},\boldsymbol{q}} \Gamma^2 \frac{\omega^2_{\boldsymbol{q}t}}{2\widetilde{\omega}_{\boldsymbol{q}t}} \coth\frac{\widetilde{\omega}_{\boldsymbol{q}t}}{2T} [(\widetilde{\varepsilon}_1(\boldsymbol{p}) - \widetilde{\varepsilon}_2(\boldsymbol{p}-\boldsymbol{q})]^{-2} \simeq \frac{\omega^2_{\boldsymbol{0}t}}{2\overline{\omega}\overline{E}} \coth\left(\frac{\overline{\omega}}{2T}\right). \quad (36)$$

Notice that due to the large band gap, the contribution of the first term in equation (34) to N_e/N is exponentially small ($N_e/N \simeq \exp(-E_g/T)$). The fact that N_e/N is not zero is entirely due to the second term, which represents the excitation of electrons by the strong interband electron–phonon coupling $\widetilde{H}^t_{e-ph}$. For non-ferroelectric crystals, where $4\Gamma^2/\overline{E} \ll 1$, this term may be negligible too. However, in our case, the threshold inequality $4\Gamma^2/\overline{E} \geqslant 1$ (equation (26)), which leads to a displacive phase transition in the system, leads, at the same time, to the finite electron density, equation (36), and, in the presence of the strong intraband electron–phonon coupling, to the spontaneous local distortions, equation (32). Notice that $\widetilde{\omega}_{qt}$ is the soft-mode frequency renormalized by the spontaneous off-centre displacements (see equation (39)). However, the correction that it introduces to N_e/N is small and therefore negligible.

Substituting equation (36) in equation (32) we finally obtain (for simplicity, $\overline{\gamma}_1 \gg \overline{\gamma}_2$, $E_p \equiv E_{p1}$)

$$|b/a_0|^2 \simeq (E_p/E_{al})\frac{\omega^2_{\mathbf{0}t}}{2\overline{\omega}\,\overline{E}}\coth\left(\frac{\overline{\omega}}{2T}\right) \tag{37}$$

where b is the magnitude of the spontaneous local off-centre displacement, a_0 is the lattice parameter and $E_{al} \equiv M^*\omega_t^2 a_0^2/2$. In section 4 we compare this calculated displacement with the displacement measured using XAFS and show that the two are in quantitative agreement.

We now want to obtain the phase transition and other properties related to it. The physical picture emerging from the above calculations is that the active ions are displaced to off-centre positions. The displacements in different cells are in different directions, and their average is zero. The ions vibrate around these new off-centre positions and the vibrations have both transverse and longitudinal branches. Equation (14) shows that these vibrations around the new positions have the same frequencies as those of the undisplaced ions—that is, they are subject to the same harmonic potential. However, due to the fact that the energy is non-linear in the displacements, we have ordinary phonon terms, spin-like terms corresponding to the off-centre displacements and interactions between them. We can now express this picture in a formal way.

We first express $\widetilde{H}$ in terms of the displacement operators $\boldsymbol{R}_{jm}$ given in equation (30), approximating the off-centre displacement term by a spin operator $b_j\sigma^z_m$, where σ^z_m is the Pauli matrix. In principle, the number of symmetry-equivalent off-centre positions in perovskites can be six, eight or twelve (for [100]-, [111]- and [110]-type displacements respectively) with the ions tunnelling or hopping among them. Using the spin operator introduces an error in the quantitative results but does not change them qualitatively. Moreover, since the ratio of the displacement to the unit-cell dimension is small, $(b/a_0)^2 \ll 1$, the quantitative error is rather small [49]. Thus the approximate displacement operator is now

$$\boldsymbol{R}_{jm} = b_j\sigma^z_m + \sum_{\boldsymbol{q},s}\sqrt{\frac{1}{2M^*\omega_{qs}N}}\,\boldsymbol{e}^j_{qs}\exp(\mathrm{i}\boldsymbol{q}\cdot\boldsymbol{m})[b_{qs} + b^+_{-qs}]. \tag{38}$$

Substituting $\boldsymbol{R}_{jm}$ in the Hamiltonian $\widetilde{H}$ we obtain the effective Hamiltonian $\widehat{H}$, which describes three interacting subsystems: electrons, (transverse polar optical) phonons and spins. As before, the strong interband electron–phonon coupling leads to transverse optical mode softening. This in turn causes the spin–phonon interaction to be large, introducing a strong indirect spin–spin interaction. It turns out that this interaction is much larger than the direct spin–spin interaction. In addition, at high temperatures, close to the transition temperature, the tunnelling frequency is negligible compared to the hopping frequency.

We shall determine the system's normal vibration spectrum in two stages. First, we shall find the full phonon and spin Green's functions $D(\boldsymbol{k}, \omega_n)$ and $S(\boldsymbol{k}, \sigma_n)$, using the Hamiltonian

$\widehat{H} - H^t_{\sigma-ph}$ only. Then, using $D(\boldsymbol{k}, \omega_n)$ and $S(\boldsymbol{k}, \sigma_n)$ as the 'free' Green's functions, we evaluate the entire-system Green's functions, including the spin–phonon interaction term $H^t_{\sigma-ph}$. In fact, this procedure corresponds to the replacement of the free Green's functions by the full (exact) ones in the inside lines of the skeleton diagrams [48].

The electron–phonon and spin–electron interactions of the Hamiltonian $\widehat{H}$ contain the operator $F_{\alpha\beta}(\boldsymbol{m}, \tau)$. Thus, as shown in the previous section, Dyson's equation cannot be used directly. Instead, it is necessary to carry out the frequency summation with respect to all ν_n (see the appendix) and only then may one introduce the effective polarization operators Π_D and Π_σ for the phonons and spins respectively.

After some transformations we obtain the soft-mode frequency (accurate to the second power of b/a_0):

$$\widetilde{\omega}^2_{0t} = \omega^2_{0t}\left[1 - \frac{4\Gamma^2}{\overline{E}} - \left(\frac{E_p}{\overline{E}}\right)^2 + \frac{3}{2}\frac{\overline{\omega}}{2\overline{E}}\coth\left(\frac{\overline{\omega}}{2T}\right) + \frac{3}{2}\left(\frac{E_a}{\overline{E}}\right)\left(\frac{b}{a_0}\right)^2\right]. \tag{39}$$

Notice that this equation is equal to equation (27) except for the last term which adds a negligible amount to $\widetilde{T}_0$ ($E_a \equiv M^*\omega^2_{qt}a^2_0$).

In the absence of the spin–phonon interaction, the frequency $\widetilde{\omega}_{qt}$ is the normal excitation frequency of the system. In the presence of this interaction, one may present the Hamiltonian $\widehat{H}$ in the form

$$\widehat{H} = \widetilde{H}_e + \overline{H} \equiv \widetilde{H}_e + \sum_q \sqrt{M^*\omega^2_{qt}a^2_0}\left(\frac{b}{a_0}\right)\sqrt{\frac{\omega_{qt}}{2N}}(b_{qt} + b^+_{-qt})\sigma^z_{-q} + \sum_q \widetilde{\omega}_{qt}b^+_{qt}b_{qt}. \tag{40}$$

The first term in $\widehat{H}$ (the pure electronic term $\widetilde{H}_e$) does not play any further role in the phase transition properties and may be omitted in the rest of this paper. The Hamiltonian $\overline{H}$ is equal to the initial Hamiltonian of the reference [37]. This Hamiltonian can be diagonalized by the shift transformation

$$\widehat{b}_{qt} = b_{qt} + \sqrt{M^*\omega^2_{qt}a^2_0}\left(\frac{b}{a_0}\right)\frac{\sigma^z_{-q}}{\widetilde{\omega}_{qt}} \tag{41}$$

and $\overline{H}$ takes the form of two non-interacting subsystems:

$$\overline{H} = -\sum_q \frac{(M^*\omega^2_{qt}a^2_0)(b/a_0)^2}{\widetilde{\omega}^2_{qt}}\sigma^z_q\sigma^z_{-q} + \sum_q \widetilde{\omega}_{qt}\widehat{b}^+_{qt}\widehat{b}_{qt} \tag{42}$$

i.e. it is an Ising-type spin Hamiltonian, but with a strongly temperature-dependent spin–spin coupling constant and the Hamiltonian of the non-interacting soft-mode branch. It is obvious that the phase transition is due to the spin subsystem only. When $T \to \widetilde{T}_0$ the spin–spin coupling constant tends to infinity. Thus, there must be a temperature $T_C > \widetilde{T}_0$ at which the system undergoes an Ising-like phase transition.

The transition temperature is determined by the coupling constant and obeys the following equation:

$$T_C = \left.\frac{(M^*\omega^2_{qt}a^2_0)(b/a_0)^2}{\widetilde{\omega}^2_{qt}(T_C)}\right|_{q=0} = \frac{\widetilde{T}_0}{2} + \frac{\sqrt{\widetilde{T}^2_0 + 4\omega^2_{0t}(E_a/A)(b/a_0)^2}}{2}. \tag{43}$$

Thus the system has a soft mode typical of a displacive-type phase transition, but experiences an order–disorder-like phase transition. The soft mode plays an unusual role as the interaction carrier: an spin–spin interaction due to the soft mode determines the spin ordering and the phase transition.

The Hamiltonian in equation (40) is equal to the Hamiltonian in equation (10) of reference [37] except that we now have explicit expressions for the local displacements and the spin–phonon coupling terms. Using this Hamiltonian, we have calculated the temperature- and frequency-dependent dielectric function [37]:

$$\epsilon(T,\omega)=\frac{e^{*2}}{M^*V_c\epsilon_0}\frac{(\mathrm{i}\omega+\nu)+2(\widetilde{\omega}_{0t}^2-\omega^2+2\mathrm{i}\omega\Gamma_D)(\nu M^*b^2/k_bT)+4\nu b|f_0|\sqrt{M^*}/k_bT}{(\mathrm{i}\omega+\nu)(\widetilde{\omega}_{0t}^2-\omega^2+2\mathrm{i}\omega\Gamma_D)-\nu\alpha_0/T}. \tag{44}$$

Here e^* and M^* are the effective charge and mass of the critical vibrational mode respectively, V_c is the cell volume, $\widetilde{\omega}_{0t}$ is the soft-mode frequency. The spin–phonon coupling is given by

$$\alpha_0=2|f_0|^2=\omega_{0t}^2E_a(b/a_0)^2. \tag{45}$$

The relaxation rate ν is loosely related to the rates of hopping among equivalent off-centre positions and its temperature dependence is given by

$$\nu=\nu_0\mathrm{e}^{-u/T} \tag{46}$$

where u is the effective potential barrier and ν_0 is the attempt rate. Finally, Γ_D is the soft-mode damping constant resulting from third- and fourth-order anharmonicities.

The ferroelectric phase transition takes place when the zero-frequency dielectric constant $\epsilon(T_C,\omega=0)$ has a pole:

$$T_C=\frac{\widetilde{T}_0}{2}+\frac{\sqrt{\widetilde{T}_0{}^2+4\alpha_0/A}}{2}. \tag{47}$$

This expression is equal to the one in equation (43).

The zero-frequency dielectric constant obeys the Curie–Weiss law

$$\epsilon(T,\omega=0)=\frac{C}{T-T_C} \tag{48}$$

with a Curie–Weiss constant

$$C=\frac{e^{*2}}{M^*V_c\epsilon_0A}\frac{1+2\widetilde{\omega}_{0t}^2M^*b^2/T}{1+|T^*|/T}\equiv C_0\left(\frac{1+2\widetilde{\omega}_{0t}^2M^*b^2/T}{1+|T^*|/T}\right) \tag{49}$$

where

$$C_0=\frac{e^{*2}}{M^*V_c\epsilon_0A} \tag{50}$$

is the Curie–Weiss constant of a purely displacive ferroelectric [2] and $|T^*|=T_C-\widetilde{T}_0$. It is easily seen that C and C_0 are equal to within a factor of order 1.

Equation (44) also predicts the existence of a central peak in a pure perovskite ferroelectric. In the frequency region where $\omega\ll\omega_{0t}$, the imaginary part of the dielectric constant can be expressed as follows:

$$\epsilon_i=\frac{\omega S\tilde{\nu}}{\omega^2+\tilde{\nu}^2}. \tag{51}$$

This expression has the form of a central peak—that is, a relaxor with a relaxation rate $\tilde{\nu}$ and intensity S, given by

$$\tilde{\nu}=\nu\frac{(T-T_C)(T+|T^*|)}{(T-\widetilde{T}_0)T}\qquad S=\frac{C(T_CT^*+\zeta\widetilde{\omega}_{0t}^2(T-\widetilde{T}_0)}{(T+T^*)(T-T_C)(T-\widetilde{T}_0)} \tag{52}$$

and $\zeta=2M^*b^2$. As $T\to T_C$ from above, the relaxation rate $\tilde{\nu}\to0$ and the intensity $S\to\infty$.

4. Comparison with experiment

In the previous section we have obtained explicit expressions for the soft-mode frequency characterized by two parameters: $\widetilde{T}_0$, the temperature at which the soft-mode frequency extrapolates to zero; and A, the soft-mode frequency squared proportionality constant. We also obtained the average of the local displacement squared b^2 and the spin–phonon coupling coefficient α_0. These results then provide the microscopic basis for the model presented in reference [37].

To check the theoretical results, we have compared the theoretical and experimental values of three important parameters: the off-centre displacement b, the transition temperature T_C and the Curie–Weiss constant C, for two materials, $KNbO_3$ and $PbTiO_3$. Both materials undergo ferroelectric transitions, but they have quite different properties. For example, in $KNbO_3$, the soft mode extrapolates to zero at about 100 K [9], i.e. far below T_C. In contrast, in $PbTiO_3$ the soft-mode extrapolates to zero at 713 K, i.e. only a few tens of degrees below T_C [11]. These three parameters are expressed in terms of six experimentally measured parameters: ω_{0t} and ω_{0l} are the average bare transverse and longitudinal phonon frequencies; they are estimated from the phonon dispersion relations excluding the zone-centre region [51] ($\omega_{0t} = 4.4 \times 10^{13}$ s^{-1}, $\omega_{0l} = 5.3 \times 10^{13}$ s^{-1} and $\omega_{0t} = 2.75 \times 10^{13}$ s^{-1}, $\omega_{0l} = 5.3 \times 10^{13}$ s^{-1} for $KNbO_3$ and $PbTiO_3$ respectively). The average gap $\overline{E}$ is estimated from the electronic band structure [52, 53] ($\overline{E} \approx 4$ eV); the polaron shift E_p is taken from optical and kinetic measurements [40, 41] ($E_p = 0.3$ eV and 0.5 eV for $KNbO_3$ and $PbTiO_3$ respectively). Notice that these experiments are not directly related to the ferroelectric transition in these crystals. The values of Γ^2 and $\overline{\omega}$ are calculated from the experimental values of A and $\widetilde{T}_0$ [9] ($\Gamma^2 = 1.04$ eV and 1.27 eV, $\overline{\omega} = 1.31 \times 10^{13}$ s^{-1} and 0.8×10^{13} s^{-1} for $KNbO_3$ and $PbTiO_3$ respectively). Using the values of these parameters, we have calculated b, T_C and C and compared them with their experimental values in table 1. The off-centre displacement b was obtained from an XAFS experiment and T_C and C were obtained from dielectric measurements. Both of these experiments are independent of the experiments that provided us with the six parameters listed above. Notice that in spite of the fact that the theory takes into account only two essential interactions, the interband and intraband electron–phonon interactions, and ignores the fine details peculiar to each material, the theoretical results are quite consistent with experiment. Using these values we get excellent agreement between the theory, as given by equations (44)–(52), and the results of various experiments.

Table 1. Calculated parameters for $KNbO_3$ and $PbTiO_3$.

Parameter	Units	$KNbO_3$, experiment	$KNbO_3$, theory	$PbTiO_3$, experiment	$PbTiO_3$, theory
b	Å	0.23	0.2	0.3	0.27
T_c	K	650	690	760	845
C	10^5 K	2.8	1.74	0.85	1.34

Two examples are shown in figures 1 and figure 2. In figure 1 we show the temperature dependence of the intensity and width of the central peak in $PbTiO_3$ [54] as compared to the values given in equations (51) and (52). In these fits the hopping rate at T_C is $\nu(T_C) = 6.3\,\mathrm{cm}^{-1}$. In figure 2 we show the imaginary part of the dielectric function of $KNbO_3$ as measured by hyper-Raman experiments [55]. The effective hopping barrier $u = 1150$ K was taken from [56]. In these fits $\Gamma_D > 70$ cm^{-1}, $\nu(T_C) = 30$ cm^{-1}.

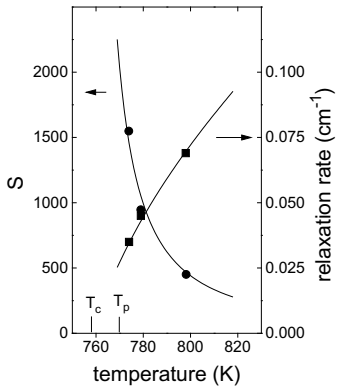

Figure 1. The integrated intensity and width of the central peak as functions of temperature. Dots: experimental results; solid curve: theoretical fit. T_p and T_c are the first-order and extrapolated second-order phase transition temperatures, respectively.

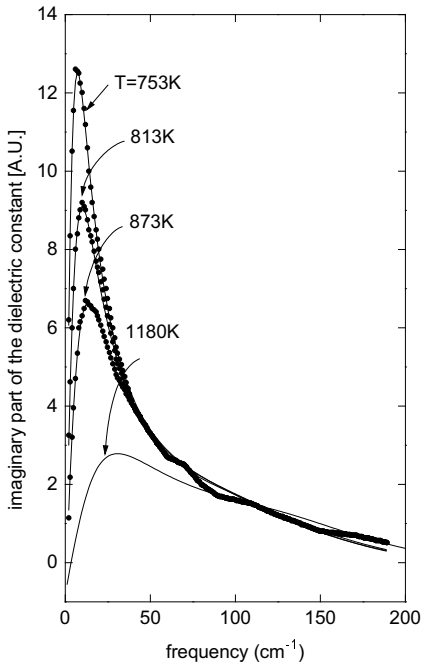

Figure 2. The imaginary part of the dielectric constant as a function of frequency for a number of temperatures. Dots: experimental results; solid curve: theoretical fit.

5. Summary and conclusions

We have presented here a self-consistent microscopic model for the ferroelectric-to-paraelectric phase transitions observed in oxygen perovskite materials. The microscopic model is based on two strong interactions: an interband electron–transverse phonon interaction that has been introduced in the past and an intraband electron–longitudinal phonon interaction introduced here for the first time. The interband electron–phonon coupling is responsible for the softening

of the lowest TO transverse phonon and the virtual excitation of electrons into the conduction band. The intraband electron–phonon interaction has only a small effect on the soft mode but it has an important effect on the virtual electrons—namely, it converts them into virtual polarons. The experimentally observed local distortions are in fact the spatial manifestation of these virtual polarons. Using modern solid-state theoretical methods, we have derived explicit analytical expressions for the soft mode and the spontaneous local distortions. Furthermore, since the Hamiltonian contains both interactions together, we are able to also calculate the interaction between the soft mode and the local distortions in terms of the electron–phonon interaction constants. Further analysis of the results showed that the off-centre displacements at different sites are coupled to each other through the soft mode and lead to the ferroelectric phase transition which is neither an ordinary displacive nor an ordinary order–disorder transition, and this finding explains in a quantitative way both the displacive-like and the order–disorder-like features of these systems. Specifically, we have provided explicit expressions for the temperature and frequency dependence of the dielectric constant and the soft mode. The results show, in agreement with experiment: that the phase transition temperature is higher and at times much higher than the temperature at which the soft mode extrapolates to zero; that the Curie–Weiss constant, in agreement with experiment, is typical of displacive-type systems in spite of the order–disorder-like features; that the off-centre displacements and their interaction with the soft mode lead naturally to a central peak and provide the temperature dependence of its intensity and width; and, finally, that the existence of off-centre displacements in some materials (for example $KNbO_3$ and $PbTiO_3$) and not in other oxygen perovskites ($SrTiO_3$ and $KTaO_3$) is strongly related to the fact that the former display polaronic mobilities while the latter do not.

To check our theoretical results we have compared the theoretical and experimental values of three important parameters: the ferroelectric–paraelectric transition temperature; the Curie–Weiss constant; and the size of the local off-centre displacements. The theoretical values were calculated using the values of a number of experimentally measured parameters. The two sets of experiments—those used to determine the first three parameters and those used to determine the other parameters—are completely independent of each other. None of the parameters were adjustable. The results show that the experimental and theoretical values of all three parameters are in good quantitative agreement.

In conclusion, we believe that the model presented here explains in a coherent quantitative way all of the main experimental facts related to the ferroelectric–paraelectric phase transition in perovskite crystals and can serve as a basis for the investigation of other structural phase transitions in the perovskite and other crystal families.

Acknowledgments

We are grateful to Professor Edward A Stern, Professor M I Klinger, Professor Boris Laihtman and Professor Leonid Shvarzman for detailed and useful discussions of this work.

Appendix

In evaluating Π in equation (23), we face the problem that Wick's theorem does not hold for the $F_{\alpha\beta}(\boldsymbol{m}, \tau)$ operators, i.e. the average of the product of any number of $F_{\alpha\beta}(\boldsymbol{m}, \tau)$ operators does not reduce to a sum of products of all possible pair averages of $F_{\alpha\beta}(\boldsymbol{m}, \tau)$ operators. This average can be expressed as a more complicated product of multiphonon correlators

$\Phi_{\alpha,\beta}(\tau_i - \tau_j) \equiv \left\langle F_{\alpha\beta}(\tau_i) F_{\beta\alpha}(\tau_j) \right\rangle$:

$$\Phi_{\alpha,\beta}(\tau_i - \tau_j) = \mathrm{e}^{-2S_{\alpha\beta}} \exp\left\{ \frac{1}{2N} \sum_{\boldsymbol{q}} \frac{|\gamma_{\boldsymbol{q}\alpha\beta}|^2}{\sinh(\omega_{\boldsymbol{q}l}/(2T))} \cosh\left[\omega_{\boldsymbol{q}l} l \left(\tau_i - \tau_j - \frac{1}{2T} r \right) \right] \right\} \tag{A.1}$$

$$\mathrm{e}^{-S_{\alpha\beta}} \equiv \left\langle F_{\alpha\beta} \right\rangle = \left\langle F_{\beta\alpha} \right\rangle = \exp\left\{ -\frac{1}{4N} \sum_{\boldsymbol{q}} |\gamma_{\boldsymbol{q}\alpha\beta}|^2 \coth \frac{\omega_{\boldsymbol{q}l}}{2T} \right\} \ll 1 \qquad \gamma_{\boldsymbol{q}\alpha\beta} \equiv (\gamma_{\boldsymbol{q}\alpha} - \gamma_{\boldsymbol{q}\beta}). \tag{A.2}$$

Indeed, a typical $2n$-order diagram for $D(\boldsymbol{q}, \omega_n)$ contains a product of electron and phonon Green's functions and the average $\Phi_{1,2n} \equiv \left\langle F_{\alpha\beta}(\tau_1) F_{\beta\alpha}(\tau_2) \cdots F_{\beta\alpha}(\tau_{2n}) \right\rangle$ of $2n$ operators $F_{\alpha\beta}(\tau_i)$, $i = 1, 2, \ldots, 2n$:

$$\begin{aligned} \Phi_{1,2n} &= \mathrm{e}^{-2nS_{\alpha\beta}} \exp\left\{ -\frac{1}{2N} \sum_{\boldsymbol{q}} \frac{|\gamma_{\boldsymbol{q}\alpha\beta}|^2}{\sinh(\omega_{\boldsymbol{q}l}/(2T))} \right. \\ &\qquad \left. \times \sum_{i,j=1, i<j}^{2n} (-1)^{i+j} \cosh\left[\omega_{\boldsymbol{q}l} \left(\tau_i - \tau_j - \frac{1}{2T} \right) \right] \right\} \\ &= \mathrm{e}^{-2nS_{\alpha\beta}} \prod_{i<j,i,j=1}^{2n} \exp\left\{ -\frac{1}{2N} \sum_{\boldsymbol{q}} \frac{|\gamma_{\boldsymbol{q}\alpha\beta}|^2}{\sinh(\omega_{\boldsymbol{q}l}/(2T))} \right. \\ &\qquad \left. \times (-1)^{i+j} \cosh\left[\omega_{\boldsymbol{q}l} \left(\tau_i - \tau_j - \frac{1}{2T} \right) \right] \right\}. \end{aligned} \tag{A.3}$$

Comparing equation (A.3) and equation (A.1) for the average of the multiphonon correlator shows that Wick's theorem is not valid for $\Phi_{1,2n}$. Equation (A.3) is the product of $(2n-1)n$ correlators of the type of equation (A.1) with different signs of the time exponent. The corresponding factors are functions of the time differences $\tau_i - \tau_j$, $i < j$, $i, j = 1, 2, \ldots, 2n$. Therefore, in the expression for $\Phi_{1,2n}$, every time τ_i is graphically connected, in the diagrams, with *all* other times τ_j, $i < j$. This qualitative difference from the corresponding expression for Wick's average leads to an important conclusion: if one associates $\Phi_{\alpha,\beta}(\tau_i - \tau_j)$ with some line in the diagrams, then all diagrams to all orders of perturbation are irreducible and therefore Dyson's equation is not soluble.

This problem can be resolved in the following way. In calculating the diagrams, it is necessary to sum over all internal electronic (ε_n) and phononic (ω_n) frequencies and over the frequencies ν_n of the multiphonon correlators $\Phi_{\alpha,\beta}(\nu_n)$ (the Fourier transform of the function $\Phi_{\alpha,\beta}(\tau_i - \tau_j)$). The actual values of the frequencies of the electron Green's functions lie near a pole, i.e. $|\varepsilon_n| \geqslant E_g/2$, whereas the actual frequencies ω_n of the phonon Green's function $D(\boldsymbol{q}, \omega_n)$ or actual frequencies ν_n of the multiphonon correlator $\Phi_{\alpha,\beta}(\nu_n)$ are considerably lower, $|\omega_n| \leqslant \omega_{\boldsymbol{q}t}$, $|\nu_n| \sim \omega_{\boldsymbol{q}l}$ (this last result was obtained by using the fact that the frequency representation for the intraband correlator, $\Phi_{\alpha\alpha}(\tau_i - \tau_j) \equiv \left\langle F_{\alpha\alpha}(\tau_i) F_{\alpha\alpha}(\tau_j) \right\rangle$ [50], is also applicable to $\Phi_{\alpha,\beta}(\nu_n)$). Therefore the temperature summation in the diagrams can be carried out for the electron and phonon Green's functions and multiphonon correlators separately. From equation (A.1) it is easily seen that

$$T \sum_{\nu_n} \Phi_{\alpha\beta}(\nu_n) = \Phi_{\alpha,\beta}(\tau)\Big|_{\tau=0} = 1. \tag{A.4}$$

Thus, after independently summing over $\nu_{n,i}$, only n terms remain in the product equation (A.3). Each of them is proportional to $\exp(2S_{\alpha\beta})$ and so a total compensation for the factor

$\exp(-2nS_{\alpha\beta}) \ll 1$ occurs in the $2n$th-order diagram and the remaining factor represents the ordinary combination of electron and phonon Green's functions only. Carrying out this procedure formally for all diagrams to all orders of perturbation, we come to the expressions that can now be associated with an ordinary sequence of reducible and irreducible diagrams. Only now can we use Dyson's equation and evaluate the polarization operator Π. The summation over internal electronic and phononic frequencies is carried out directly in the diagrams for the polarization operator.

The polarization operator diagrams can now be obtained in just the same way as for conventional interband theory of (displacive-type) ferroelectrics. The only difference is that the ordinary electronic spectrum $\varepsilon_\alpha(\boldsymbol{p})$ is replaced by the polaronic spectrum $\widetilde{\varepsilon}_\alpha(\boldsymbol{p})$.

References

[1] Lines M E and Glass A M 1977 *Principles and Applications of Ferroelectrics and Related Materials* (Oxford: Clarendon)
[2] Vaks V G 1973 *Introduction to the Microscopic Theory of Ferroelectricity* (Moscow: Nauka) (in Russian)
[3] Comes R, Lambert M and Guinier A 1970 *Acta Crystallogr.* A **26** 244
[4] Comes R, Currat R, Denoyer F, Lambert M and Quittet A M 1976 *Ferroelectrics* **12** 3
[5] Comes R and Shirane G 1972 *Phys. Rev.* B **5** 1886
[6] Quittet A M and Lambert M 1973 *Solid State Commun.* **12** 1053
[7] Yacoby Y and Just S 1974 *Solid State Commun.* **15** 715
[8] Yacoby Y 1978 *Z. Phys.* B **31** 275
[9] Fontana M D, Metrat G, Servoin J L and Gervais F 1984 *J. Phys. C. Solid State Phys.* **16** 483
[10] Scott J F 1974 *Rev. Mod. Phys.* **46** 83
[11] Axe J D, Harada J and Shirane G 1970 *Phys. Rev.* B **1** 1227
[12] Fontana M D, Idrissi H, Kugel G E and Wojcik K 1991 *J. Phys.: Condens. Matter* **3** 8695
[13] Shapiro S M, Axe J D and Shirane G 1972 *Phys. Rev.* B **6** 4332
[14] Sicron N, Ravel B, Yacoby Y, Stern E A, Dogan F and Rehr J J 1994 *Phys. Rev.* B **50** 13 168
[15] Kim K H, Elam W T and Skelton E F 1990 *Mater. Res. Soc. Symp. Proc.* **172** 291
[16] de Mathau N, Prouzet E, Hasson E and Dexpert H 1993 *J. Phys.: Condens. Matter* **5** 1261
[17] Nishihata Y, Kamishima O, Ojima K K, Sawada A, Maeda H and Terauchi H 1994 *J. Phys.: Condens. Matter* **6** 9317
[18] Hanske-Petitpierre O, Yacoby Y, Mustre de Leon J, Stern E A and Rehr J J 1991 *Phys. Rev.* B **44** 6700
[19] Zkharov A and Yacoby Y, unpublished
[20] Sicron N, Yacoby Y, Stern E A and Dogan F 1997 *Proc. 9th Int. XAFS Conf. (1996); J. Physique Coll. IV* C **2** 1047
[21] Rechav B, Yacoby Y, Stern E A, Rehr J J and Newville M 1994 *Phys. Rev. Lett.* **72** 1352
[22] Bilz H, Benedek G and Bussman-Holder A 1987 *Phys. Rev.* B **35** 4840
[23] Bilz H, Bussman A, Benedek G, Buffner H and Strauch D 1980 *Ferroelectrics* **25** 339
[24] Perry G, Currat R, Buhay H, Migoni R, Stirling W and Axe J 1989 *Phys. Rev.* B **39** 8666
[25] Bersuker I B 1989 *Vibronic Interaction in Molecules and Crystals (Springer Series in Chemical Physics vol 49)* (Berlin: Springer)
[26] Kristoffel N N and Konsin P 1988 *Phys. Status Solidi* b **149** 11 and references therein
[27] Girshberg Ya G and Tamarchenko V I 1976 *Fiz. Tverd. Tela* **18** 1066 (Engl. Transl. 1976 *Sov. Phys.–Solid State* **18** 609)
Girshberg Ya G and Tamarchenko V I 1976 *Fiz. Tverd. Tela* **18** 3340 (Engl. Transl. 1976 *Sov. Phys.–Solid State* **18** 1946)
[28] Girshberg Ya G, Bursian E V and Tamarchenko V I 1978 *Ferroelectrics* **18** 39
[29] Bersuker I B 1966 *Phys. Lett.* **20** 589
[30] Stachiotti M, Dobry A, Migoni R and Bussman-Holder A 1993 *Phys. Rev.* B **47** 2473
[31] Bussman-Holder A 1996 *J. Phys. Chem. Solids* **57** 1445
[32] Cohen R E and Krakauer H 1990 *Phys. Rev.* B **42** 6416
[33] Postnikov A V, Neumann T, Borstel G and Methfessel M 1993 *Phys. Rev.* B **48** 5910
[34] King-Smith R D and Vanderbilt D 1994 *Phys. Rev.* B **49** 5825
[35] Zhong W, Vanderbilt D and Rabe K M 1995 *Phys. Rev.* B **52** 6301
[36] Waghmare U V and Rabe K M 1997 *Phys. Rev.* B **55** 6161

[37] Girshberg Ya and Yacoby Y 1997 *Solid State Commun.* **103** 425
[38] Bursian E V, Girshberg Ya G and Starov E N 1971 *Phys. Status Solidi* b **46** 529
[39] Mahgereften D, Kirilov D, Cudney R S, Bacher G D, Pierce R M and Feinberg J 1996 *Phys. Rev.* B **53** 7094
[40] Bursian E V, Girshberg Ya G and Ruzhnikov A V 1976 *Phys. Status Solidi* b **74** 689
[41] Bernasconi P, Biaggio I, Zgonik M and Gunter P 1997 *Phys. Rev. Lett.* **78** 106
[42] Wemple S H, DiDomenico M Jr and Jayaraman A 1969 *Phys. Rev.* **80** 547
[43] Wemple S H 1965 *Phys. Rev.* **137** A1575
[44] Firsov Yu A (ed) 1975 *Polarons* (Moscow: Nauka)
[45] Lang I G and Firsov Yu A 1962 *Zh. Eksp. Teor. Fiz.* **43** 1843 (Engl. Transl. 1963 *Sov. Phys.–JETP* **16** 1301)
[46] Alexandrov A S and Mott N F 1995 *Polarons and Bipolarons* (Singapore: World Scientific)
[47] Aronov A G and Kudinov E K 1968 *Zh. Eksp. Teor. Fiz.* **55** 1344 (Engl. Transl. 1969 *Sov. Phys.–JETP* **28** 704)
[48] Abrikosov A A, Gorkov L P and Dzyaloshinski I E 1975 *Methods of Quantum Field Theory in Statistical Physics* (Englewood Cliffs, NJ: Prentice-Hall)
[49] Vaks V G and Larkin A I 1965 *Zh. Eksp. Teor. Fiz.* **49** 975 (Engl. Transl 1966 *Sov. Phys.–JETP* **22** 678)
[50] Alexandrov A and Capellmann H 1991 *Phys. Rev.* B **43** 2042
[51] Bilz H and Kress W 1979 *Phonon Dispersion Relations in Insulators (Springer Series in Solid-State Sciences vol 10)* (Berlin: Springer)
[52] Wiesendanger E 1974 *Ferroelectrics* **6** 263
[53] *Landolt–Börnstein New Series* 1981 Group III, vol 16a, ed K-H Hellwege (Berlin: Springer)
[54] Fontana M D, Idrissi H and Wojcik K 1990 *Europhys. Lett.* **11** 419
[55] Vogt H, Fontana M D, Kugel G F and Gunter P 1986 *Phys. Rev.* B **34** 410
[56] Sokolov J P, Chase L L and Rytz D 1988 *Phys. Rev.* B **38** 597